ELSEVIER

Journal of Chromatography A, 781 (1997) 23–34

JOURNAL OF CHROMATOGRAPHY A

Prediction of the migration behavior of analytes in capillary electrophoresis based on three fundamental parameters

Philip Britz-McKibbin, David D.Y. Chen*

Department of Chemistry, University of British Columbia, Vancouver, BC V6T 1Z1, Canada

Abstract

The prediction of analyte migration behavior in capillary electrophoresis (CE) is essential for rapid method development. The dynamic complexation model, based on 1:1 interactions, was used to accurately predict the apparent electrophoretic mobilities and the migration times of a group of deoxyribonucleotides (dNPs) at various concentrations of β-cyclodextrin (β-CD). The electrophoretic mobility of the analyte, the electrophoretic mobility of the analyte–additive complex and the equilibrium constant are the three fundamental parameters required to determine the mobility of an analyte. The apparent migration time of the analyte can be predicted once the electroosmotic mobility and relative viscosity of the solution are known. Optimum separation conditions can be determined based on these parameters. Excellent agreement between observed analyte migration behavior and predicted values was demonstrated, with relative errors being often less than 1%. The theory was tested repeatedly under various conditions in order to assess its predictive capabilities and limitations. Analysis by molecular modeling, in conjunction with calculated electrophoretic parameters and equilibrium constants, provided deeper insight into the probable mechanisms of the separation process at the molecular level. © 1997 Elsevier Science B.V.

Keywords: Deoxyribonucleotides; Migration behaviour; Migration time prediction

1. Introduction

One of the inherent advantages of CE is the ease with which the composition of the background electrolyte can be adjusted in order to modify the analyte mobility. The use of additives in CE has led to dramatic increases in separation power. Micelles, complexing agents, affinity ligands and ion pairing agents are various types of additives that have been used to control the selectivity of the separation. Systematic optimization using one or more additives, based on the fundamental understanding of the determinants of migration behavior, would represent a significant advancement in CE.

In chromatography, the migration behavior of an analyte is primarily determined by the velocity of the mobile phase and the fraction of analyte in the mobile phase, because the velocity of the stationary phase is zero. However, in CE separations that utilize additives in the background electrolyte, the analyte mobility is determined by three parameters [1–5]: the electrophoretic mobilities of the free and complexed analyte, and the equilibrium constant of the analyte–additive interaction. If the viscosity of the background electrolyte changes when an additive is used, a viscosity correction factor has to be included to avoid obscuring the effect of the shift in equilibrium on the measured mobilities. It is often sufficient in chromatography to concentrate on improving the resolution of the most difficult pair of analytes for the optimization of separation conditions. Whereas in CE, because the mobility of an analyte is controlled

*Corresponding author.

0021-9673/97/$17.00
PII S0021-9673(97)00484-6

by the three parameters, the optimum conditions depend not only on specific pairs of analytes, but also on the migration behavior of other analytes. For a complicated mixture, it is essential to model the migration behavior of all analytes before optimum conditions can be predicted.

Since the first description of CE with additives by Terabe and co-workers [6], there have been several theoretical models developed for specific additive types. Models to describe chiral separations [1–3,7–12], affinity CE [13], complexation CE [14,15] and micellar CE [16–19] have been described. Our group has amalgamated and extended the existing theories by proposing to use the theory based on dynamic complexation between analytes and additives to describe the migration behavior of all types of open tubular CE [4].

There have only been a few reports devoted to the prediction of analyte migration behavior. Khaledi and co-workers [20,21] utilized an empirical/semi-empirical model to predict mobilities and migration times. This type of approach can be used for rapid separation optimization based on a limited set of experimental conditions. Wren et al. [1] developed a theoretical model based on physicochemical parameters to describe and optimize chiral separations. The model was supported by experimental results and provided a systematic way to optimize the additive concentration to achieve maximum resolution between enantiomers. Similar models for chiral separations have been expanded by Goodall et al. [3,7,8] and Sepaniak et al. [9] to optimize chiral separations for enantiomeric drugs and amino acids, respectively. The dynamic complexation model can be applied to the separation of all types of analytes (charged or neutral, chiral separations, etc.), in all types of background electrolytes (aqueous or nonaqueous), with any number of additives [4,5].

The aim of this paper is to examine the generality of this theoretical model by describing the migration behavior of 12 deoxyribonucleotides using β-CD as the additive. An extensive study of the predictive capabilities of the model under a variety of constraints is investigated in order to assess its strengths and limitations. In addition, molecular modeling of analyte–additive interactions is used to confirm the trends observed in the equilibrium constants obtained experimentally.

2. Background

For a 1:1 analyte–additive interaction [4], the electrophoretic mobility of an analyte is described by:

$$\nu\mu_{ep}^{A} = \frac{1}{1+k'}\mu_{ep,A} + \frac{k'}{1+k'}\mu_{ep,AC} \quad (1)$$

where ν is the viscosity correction factor ($\nu=\eta/\eta^0$, the viscosity with the additive compared with the viscosity without the additive), k' is the capacity factor which is equal to K[C] (K is the equilibrium constant of the analyte–additive interaction and [C] is the additive concentration), μ_{ep}^{A} is the apparent electrophoretic mobility of the analyte and $\nu\mu_{ep}^{A}$, $\mu_{ep,A}$ and $\mu_{ep,AC}$ are the ideal state electrophoretic mobilities of the analyte, free analyte and the analyte–additive complex, respectively. The ideal state refers to conditions where the additive concentration is approaching zero.

Because the three parameters are intrinsic properties of the analyte–additive pair in a defined system, the electrophoretic mobility of an analyte is a function of additive concentration only. Once the values of these three parameters are known and the viscosity effect is taken into account, the migration behavior of the analyte can be predicted for all additive concentrations. However, it is important to realize that these parameters could be affected by temperature as well. Goodall et al. [22] reported that the neglect of viscosity and temperature corrections combine to underestimate K significantly. The use of a thermostatted CE instrument, that is operated at a low enough voltage to minimize Joule heating, will increase the accuracy and the precision of the parameters.

The mobility of the free analyte, $\mu_{ep,A}$, can be determined directly by measuring the mobility without any additive present. However, the values of K and $\mu_{ep,AC}$ must be obtained from the regression analysis using the measurements of the apparent mobility of the analyte at various concentrations of additive. Eq. (1) can be transformed into various linear equations for the calculation of K and $\mu_{ep,AC}$. Recently, various plotting methods used to determine binding constants, which included nonlinear curve fitting and three linear plotting methods (double reciprocal, y-reciprocal and x-reciprocal plots) have

been discussed for both aqueous and nonaqueous CE [5,23]. Theoretically, the various plotting methods should give identical results. In practice, the results may vary because of the way that errors associated with the variables are transformed. Although the equilibrium constant can be calculated using nonlinear regression [1,3,9], the linear presentation of data can be useful for detecting trends and deviations from the presumed stoichiometry of the interactions [24]. Bowser et al. compared these plotting methods in a nonaqueous buffer system [5]. Eq. (1) can be rearranged to:

$$\frac{[C]}{(\nu\mu_{ep}^{A} - \mu_{ep,A})} = \frac{[C]}{(\mu_{ep,AC} - \mu_{ep,A})} + \frac{1}{(\mu_{ep,AC} - \mu_{ep,A})K} \quad (2)$$

A plot of $[C]/(\nu\mu_{ep}^{A} - \mu_{ep,A})$ versus [C] should give a straight line, therefore, the values of $\mu_{ep,AC}$ and K can be obtained from the slope and the intercept, respectively. Once these values are determined, the ideal state mobility of an analyte can be calculated by substituting the values into Eq. (1). However, in order to compare these theoretical values with the measured values, the viscosity correction factor has to be incorporated [4,5]. The migration times of the analytes can then be calculated once the electroosmotic mobility has been measured. The optimum additive concentration(s) occurs where there is the least overlap in the analyte mobility curves.

3. Experimental

3.1. Apparatus

All experiments were performed on a Beckman P/ACE 5500 automated CE system using System Gold software (Beckman) with a 386 PC computer. Fused silica capillaries (Polymicro Technologies, Phoenix, AZ, USA) with inner diameters of 50 μm, outer diameters of 375 μm, and lengths of 27, 37 and 47 cm were used. New capillaries were first rinsed with 0.1 *M* NaOH for 3 min, then rinsed with deionized water for 5 min and finally washed with a 160 m*M* borate buffer, pH 9.0, for 10 min and equilibrated overnight before being used. The sample was introduced using a pressure injection for 3 s. All separations were carried out at 20°C, and the UV absorption was monitored at 254 nm. Voltages of 5, 6.85 and 8.7 kV were used with the 27, 37 and 47 cm capillaries, respectively, maintaining a relative electric field of 185 V/cm. Relative viscosity measurements were performed by a 2 s injection of a 1% benzene plug onto the capillary inlet, UV detection at 214 nm using a 57 cm capillary, and measuring the time needed to push the plug to the detector under a constant pressure of 20 p.s.i. (1 p.s.i. = 6894.76 Pa). Molecular modeling was performed on CS Chem 3D version 3.2 (CambridgeSoft Corporation, Cambridge, USA). Molecular structures were originally drawn on CS ChemDraw version 3.5 and their structures minimized on CS Chem 3D. Complexation of the deoxyribonucleotides with β-CD was studied using molecular modeling by successively minimizing the energy of the complex, then running a molecular dynamics program and repeating this procedure until an energy minimum was observed. Energy minima are determined by both steric and noncovalent intermolecular forces of dipole/dipole, charge/dipole and Van der Waal forces. Solvation effects and charge (electrostatic) interactions are neglected in the modeling.

3.2. Chemicals and procedures

Borax ($Na_2B_4O_7 \cdot 10H_2O$), β-CD (cycloheptaamylose) and the 2′-deoxyribonucleotides: deoxyadenosine mono-, di- and triphosphate (dAMP, dADP and dATP), deoxyguanosine mono-, di- and triphosphate (dGMP, dGDP and dGTP), deoxycytosine mono-, di- and triphosphate (dCMP, dCDP and dCTP) and deoxyuridine mono-, di- and triphosphate (dUMP, dUDP and dUTP), were all purchased from Sigma (St. Louis, MO, USA). HPLC grade methanol was purchased from Fisher Scientific (Nepean, ON, Canada). Stock solutions of 160 m*M* borate were prepared in deionized water. A stock solution of 20 m*M* β-CD was prepared by dissolving the appropriate amount of β-CD in borate buffer. The appropriate volumes of stock solutions were mixed with buffer to make the 160 m*M* borate (pH 9.0) with concentrations of β-CD ranging from 5 to 20 m*M*. A stock solution of the analytes was

prepared by dissolving approximately equal concentrations ($1 \cdot 10^{-3}$ M) of each deoxyribonucleotide in deionized water. This stock solution was further diluted to a concentration of approximately $5 \cdot 10^{-5}$ M before injection onto the capillary. Methanol (1.7%, v/v) was used as the EOF marker in the sample. Peaks were identified by spiking the sample solution with standard solutions of each deoxyribonucleotide. Before experiments were started, an Ohm plot was performed with the 27 cm capillary and the run buffer in order to select a voltage at which Joule heating was minimal. This was necessary to ensure the heat generated during the separation was efficiently dissipated. A voltage of 5 kV was used and this voltage was well within the linear region of the Ohm plot.

4. Results and discussion

4.1. Determination of the three parameters and their influence on the separation

Fig. 1 shows the effect of changes in the β-CD concentration on the migration behavior of the analytes. When no additive is used, only ten resolved peaks can be observed for the twelve dNPs. The negative electrophoretic mobility of the nucleotides generally increases from mono- to di- to triphosphate. However, for a given degree of phosphorylation, the dNPs of guanine and uridine show larger negative electrophoretic mobilities when compared to the similarly sized dNPs of adenine and cytosine, respectively. Both guanine and uridine have an acidic hydrogen ($pK_a \approx 9.5$) [25] that is partially ionized in the borate buffer (pH 9.0). Thus, the absolute value of $\mu_{ep,A}$ generally increases with increasing phosphorylation in the order U>C>G>A. When 5 mM additive is used in the buffer, significant changes in the migration order of the dNPs is observed. By analyzing the changes in the migration times of the analytes with changes in cyclodextrin concentration, it can be seen that the dNPs of adenine exhibit the most dramatic decreases in the migration time, compared to slow decreases in migration time for the dNPs of guanine, uridine, or cytosine. These trends can be explained by Eq. (1) using the $\mu_{ep,A}$, $\mu_{ep,AC}$ and K values.

It was observed that the data points were increasingly nonlinear, using Eq. (2), for weakly binding analytes ($K<10$). The nonlinearity is a result of the limited range of the fraction of analyte in the complex form. Ideally, the fraction of analyte complexed with an additive (f_{AC}) should range from 0.2 to 0.8 in order to minimize the error during the calculation process [5]. To meet this requirement, the concentration of β-CD should change from 20 to 80 mM, when the K value is 10 M^{-1}. Unfortunately, the limited solubility of β-CD in aqueous solution restricts the upper limit of the concentration to 20 mM, so a concentration range varying from 7.5 to 20 mM β-CD was used for the calculation. In cases where it is impossible to obtain the parameters directly from a linear regression, reasonable estimates for K and $\mu_{ep,AC}$ were used. Comparison of the values of K and $\mu_{ep,AC}$ obtained without viscosity correction to the measured mobilities shows not only a significant underestimation of the K values (varying up to 60% for weakly binding analytes), but also some unrealistic values for the complex mobilities (which are either seriously underestimated, or result in positive mobilities for weakly binding analytes, see Table 1).

Table 1 shows the values of $\mu_{ep,A}$, K and $\mu_{ep,AC}$ for each analyte. Distinct trends can be seen in the magnitudes of the binding constants and complex mobilities which can readily explain the observed migration behavior of the analytes in the electropherograms of Fig. 1. To compare the effect of complexation on analytes with different values of $\mu_{ep,A}$, the difference in mobility ($\mu_{ep,AC} - \mu_{ep,A}$) or the relative change in mobility ($\mu_{ep,AC} - \mu_{ep,A})/\mu_{ep,A}$ can be used. The analytes differ in the structure of the base and the degree of phosphorylation. The base on the nucleotide significantly influences the magnitude of the binding constant. Nucleotides with adenine bases show the largest affinity for β-CD (dAMP has the largest K, 63.8 M^{-1}). The dNPs of guanine and uridine have similar, yet lower affinities towards β-CD, while the dNPs of cytosine have extremely weak interactions.

These calculated K values are consistent with the measurements of the binding constants of ribonucleotides with β-CD made by Formoso [26] using circular dichroism and Hoffman and Bock [27] using UV absorption spectroscopy. Steric effects and the

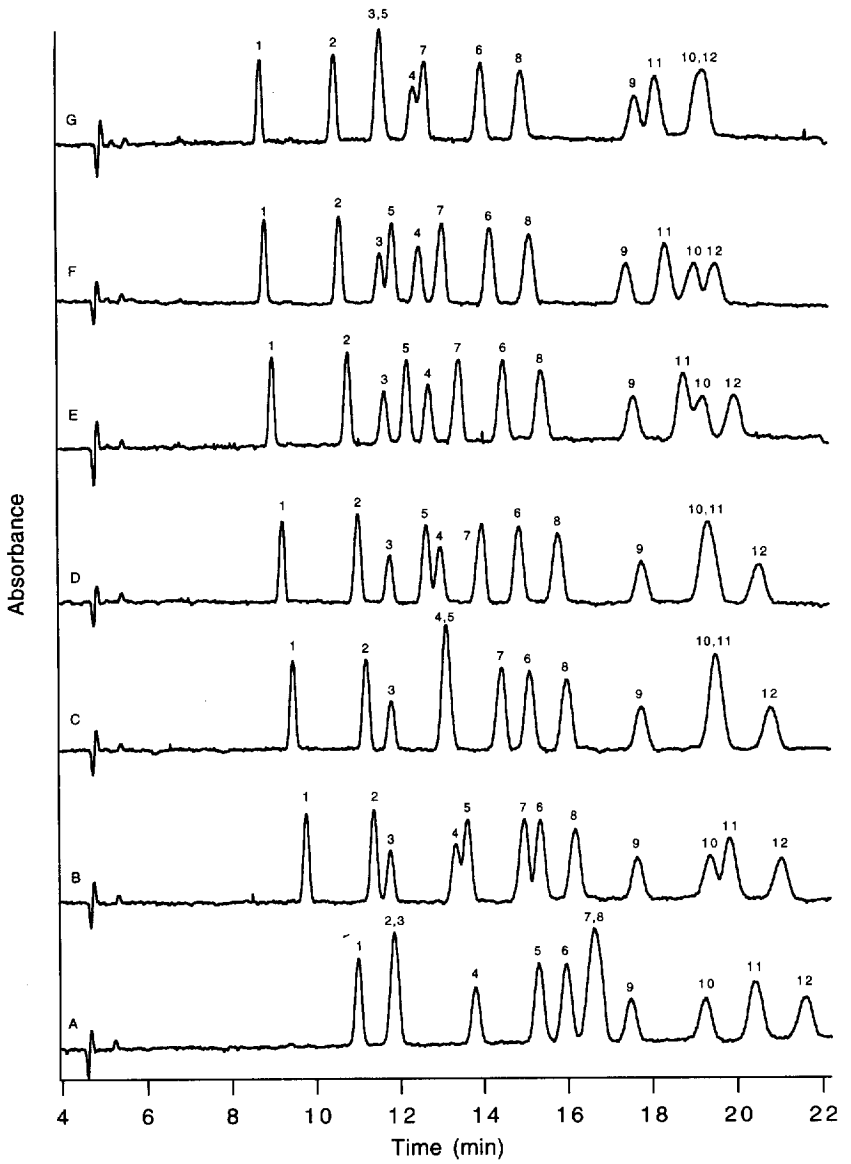

Fig. 1. Series of electropherograms at various concentrations of β-CD: A = 0 m*M*, B = 5 m*M*, C = 7.5 m*M*, D = 10 m*M*, E = 12.5 m*M*, F = 15 m*M* and G = 20 m*M*. Deoxyribonucleotides: 1 = dAMP, 2 = dGMP, 3 = dCMP, 4 = dUMP, 5 = dADP, 6 = dGDP, 7 = dATP, 8 = dGTP, 9 = dCDP, 10 = dCTP, 11 = dUDP and 12 = dUTP. The buffer used in these runs is 160 m*M* borate with a pH of 9.0.

functional groups on the bases can be used to rationalize the observed trend. Molecular models show that the pyrimidine bases of U and C are too small for significant interactions to occur within the apolar cyclodextrin cavity [27]. Adenine was found to have a greater affinity towards β-CD than the larger guanine because insertion of guanine leads to distortion of the cyclodextrin cavity. The acidity of the guanine base can also explain the decreased binding affinity towards cyclodextrin compared to the neutral adenine base. However, it is not clear why U has a greater affinity than C. The magnitude of the interaction between the dNPs and β-CD is also dependent on the degree of phosphorylation, with

Table 1
Determination of the fundamental parameters influencing the mobility

Analyte	K (M^{-1})	K^a (M^{-1})	$\mu_{ep,A}\times10^{-3}$ ($cm^2\ V^{-1}\ s^{-1}$)	$\mu_{ep,AC}\times10^{-3}$ ($cm^2\ V^{-1}\ s^{-1}$)	$\mu_{ep,AC}-\mu_{ep,A}$	Rel. mobility change[c] (%)	$\mu_{ep,A}/\mu_{ep,AC}$ ($\mu_{ep,A}/\mu^d_{ep,AC}$)	$\mu^a_{ep,AC}\times10^{-3}$ ($cm^2\ V^{-1}\ s^{-1}$)	$\mu^d_{ep,AC}\times10^{-3}$ ($cm^2\ V^{-1}\ s^{-1}$)
dAMP	63.8±1.4	52.6±1.0	−0.2241±0.0004	−0.123±0.002	0.101	−45.2	1.83 (2.70)	−0.093±0.001	−0.0831
dGMP	18.2±1.6	14.0±1.0	−0.2359±0.0004	−0.116±0.010	0.120	−50.8	2.03 (2.63)	−0.030±0.002	−0.0896
dCMP	8.4±4.0	4.6±1.6	−0.2359±0.0004	−0.136±0.031	0.100	−42.3	1.73 (2.81)	+0.106±0.038	−0.0838
dUMP	18.6±2.4	12.3±1.2	−0.2572±0.0004	−0.164±0.021	0.093	−36.2	1.57 (2.81)	−0.055±0.005	−0.0915
dADP	34.5±1.3	27.3±1.0	−0.2701±0.0005	−0.150±0.005	0.121	−44.6	1.81 (2.42)	−0.091±0.003	−0.1117
dGDP	11.9±2.2	8.0±1.2	−0.2748±0.0004	−0.144±0.027	0.131	−47.6	1.91 (2.37)	+0.023±0.011	−0.1158
dATP	24.9±1.6	19.5±1.1	−0.2793±0.0003	−0.147±0.009	0.133	−47.5	1.79 (2.22)	−0.069±0.006	−0.1256
dGTP	10.1±2.8	6.3±1.3	−0.2793±0.0003	−0.156±0.043	0.123	−44.1	1.79 (2.19)	+0.054±0.029	−0.1276
dCDP	5.3±4.0	0.8±1.0	−0.2847±0.0004	−0.217±0.092	0.068	−23.8	1.31 (2.50)	−1.226±0.033	−0.1140
dCTP	5.0[b]	<5.0	−0.2941±0.0004	−0.218[b]	0.076	−25.9	1.35 (2.28)	–	−0.1290
dUDP	8.6±3.2	4.6±1.4	−0.2994±0.0004	−0.174±0.064	0.125	−41.9	1.72 (2.49)	+0.128±0.036	−0.1200
dUTP	7.2±3.2	2.2±1.5	−0.3042±0.0004	−0.169±0.073	0.135	−44.4	1.80 (2.28)	+0.522±0.042	−0.1336

[a] Values of K and $\mu_{ep,AC}$ calculated without using the viscosity correction factor ν.
[b] Approximated values used for prediction (dCTP).
[c] Relative mobility change $=-[\mu_{ep,AC}-\mu_{ep,A}]/\mu_{ep,A}\times100$.
[d] Estimated $\mu_{ep,AC}$ determined using Eq. (3).

monophosphorylated dNPs exhibiting the largest affinity. The association constant is observed to be drastically reduced going from mono- to diphosphates (up to a 50% reduction in K values), while the difference between di- to triphosphates is less substantial. Increasing the phosphorylation of each nucleotide increases the charge and the solvation sphere, resulting in a weaker interaction with the apolar cavity of β-CD. Consequently, the magnitude of K is observed to decrease dramatically from mono- to diphosphates. The much less significant decrease in K between the di- and triphosphates can be explained by comparing the relative changes in the free mobilities. Despite an overall increase in the charge of the analyte from di- to triphosphates, the relative increase in mobility is significantly lower than from mono- to diphosphates. For example, for the nucleotide series dGMP, dGDP and dGTP, the $\mu_{ep,A}$ are −0.2359, −0.2748 and −0.2793 ($\times10^{-3}$ $cm^2\ V^{-1}\ s^{-1}$), while the K values are 18.2, 11.9 and 10.1, respectively. This suggests that the di- and triphosphates have comparable charge to size ratios. This trend is supported by work done by Uhrova et al. [28] which demonstrated that the ionization of nucleoside triphosphates is incomplete due to the weaker acidity of the terminal OH groups of polyphosphates.

The net mobility of an analyte is also dependent on the magnitude of $\mu_{ep,AC}$. Although the differences in the K values have generally been considered as the most dominant factor in separations, a comparison of the K values for dGMP and dUMP demonstrate that even when the K values are similar, separation can still be achieved if the complex mobilities ($\mu_{ep,AC}$) or the changes in mobilities ($\mu_{ep,AC}-\mu_{ep,A}$) are different. This property demonstrates the fundamental difference between CE and chromatography. However, it is important to note that there is no direct relationship between the K values and the complex mobilities. The affinity of the analyte for this additive is determined by both steric factors and the strength of the hydrophobic interactions. The value of $\mu_{ep,AC}$ is determined by the overall shape of the complex, assuming negligible changes in the charge of the analyte upon complexation. For instance, although dAMP and dGMP have drastically different values for K, their complex mobilities are quite similar. In contrast, dGMP and dUMP, which have similar binding affinities to β-CD, possess significantly different values for $\mu_{ep,AC}$. Another way to investigate the nature of the interaction between an analyte and an additive, as suggested by Goodall and co-workers [22], is to use the ratio of $\mu_{ep,AC}/\mu_{ep,A}$ as a measure of the relative change in hydrodynamic radius (Stoke's radius). Again, a similar trend is observed with respect to the

type of nucleotide base and the degree of phosphorylation.

Table 1 also shows the values of the complex mobility estimated by:

$$\mu_{ep,AC} \approx \left(\frac{M_A}{M_{AC}}\right)^{2/3} \mu_{ep,A} \quad (3)$$

where M_A and M_{AC} are the molecular masses of the analyte and additive, respectively, and $M^{2/3}$ is a measure of the surface area of the molecule [29,30]. This type of simplified estimation of the complex mobility neglects the important effects of solvation in aqueous solutions. A comparison of the $\mu_{ep,AC}$ values calculated by Eq. (3) with the experimentally determined values of $\mu_{ep,AC}$ clearly demonstrates that by neglecting solvation effects on the overall size of the analyte–additive complex, the complex mobility is significantly underestimated, resulting in an overestimated $\mu_{ep,A}/\mu_{ep,AC}$. Moreover, estimation of complex mobilities by molecular masses cannot take specific steric effects into account. Therefore, the complex mobilities must be determined experimentally until a more rigorous theory is available.

4.2. Computer modeling of the molecular inclusion complexes

Computer modeling of inclusion complexes may indicate the most probable binding orientation upon complexation, and can be used to estimate the change in free energy [9]. The complex formation of dAMP and dCMP with β-CD were modeled based on noncovalent interactions while neglecting the effects of charge interactions and solvation. dAMP and dCMP were best suited for modeling because their bases are electrically neutral and were observed to exhibit widely different affinities. A comparison of the complexation of dAMP and dCMP with β-CD revealed that the most stable configuration for dAMP is when the adenine base is located within the apolar cavity of β-CD, while the cytosine base of dCMP is most stable when located outside the cavity, along the rim of the cyclodextrin (see Fig. 2). This observation supports previous arguments regarding ribonucleotide affinities for cyclodextrin given by Hoffman and Bock [27]. Since the relative size and hydrophobicity of the base are the most important factors determining the strength of binding, clearly

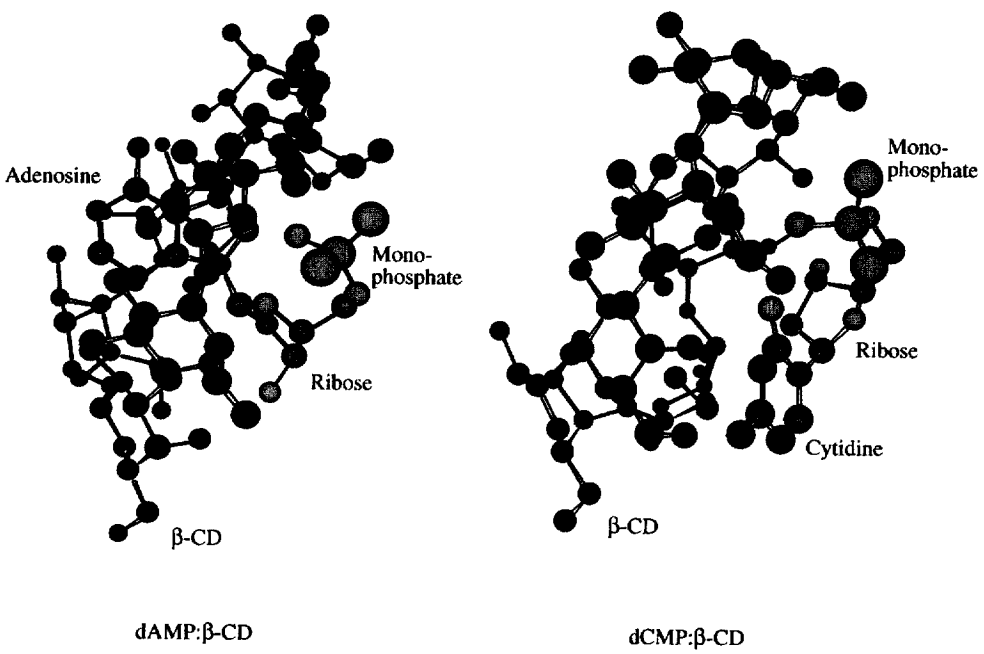

Fig. 2. 3-D computer molecular models of the lowest energy configurations of the inclusion complexes: dAMP:β-CD and dCMP:β-CD.

dAMP demonstrates a greater affinity for β-CD than dCMP, which is also confirmed experimentally.

4.3. Prediction of analyte migration behavior

Incorporation of the three fundamental parameters into Eq. (1) should be able to describe the nonlinear change of analyte mobility at various additive concentrations. Fig. 3 depicts the predicted ideal state electrophoretic mobilities of the 12 deoxyribonucleotides (solid lines) as a function of β-CD concentration by using the values of $\mu_{ep,A}$, $\mu_{ep,AC}$ and K from Table 1. There is excellent correlation between the calculated values and the experimentally measured mobilities with a relative error of less than 1%. The mobility of dAMP ($K=63.8$, $\mu_{ep,AC}=-0.1227\cdot 10^{-3}$ cm^2 V^{-1} s^{-1}) drastically changes with cyclodextrin concentration. In contrast, the mobilities of weakly interacting analytes, such as dCMP, dCDP and dCTP, change minimally with increasing concentration of additive. This type of plot gives an overview of all possible mobilities for each analyte, showing the additive concentration(s) where the overlap of the analyte mobilities is the least. For example, dGMP–dCMP and dATP–dGTP are overlapping peaks without additive, but they are separated at higher concentrations of β-CD due to the differential interaction with the neutral additive. Moreover, the actual order of migration may change

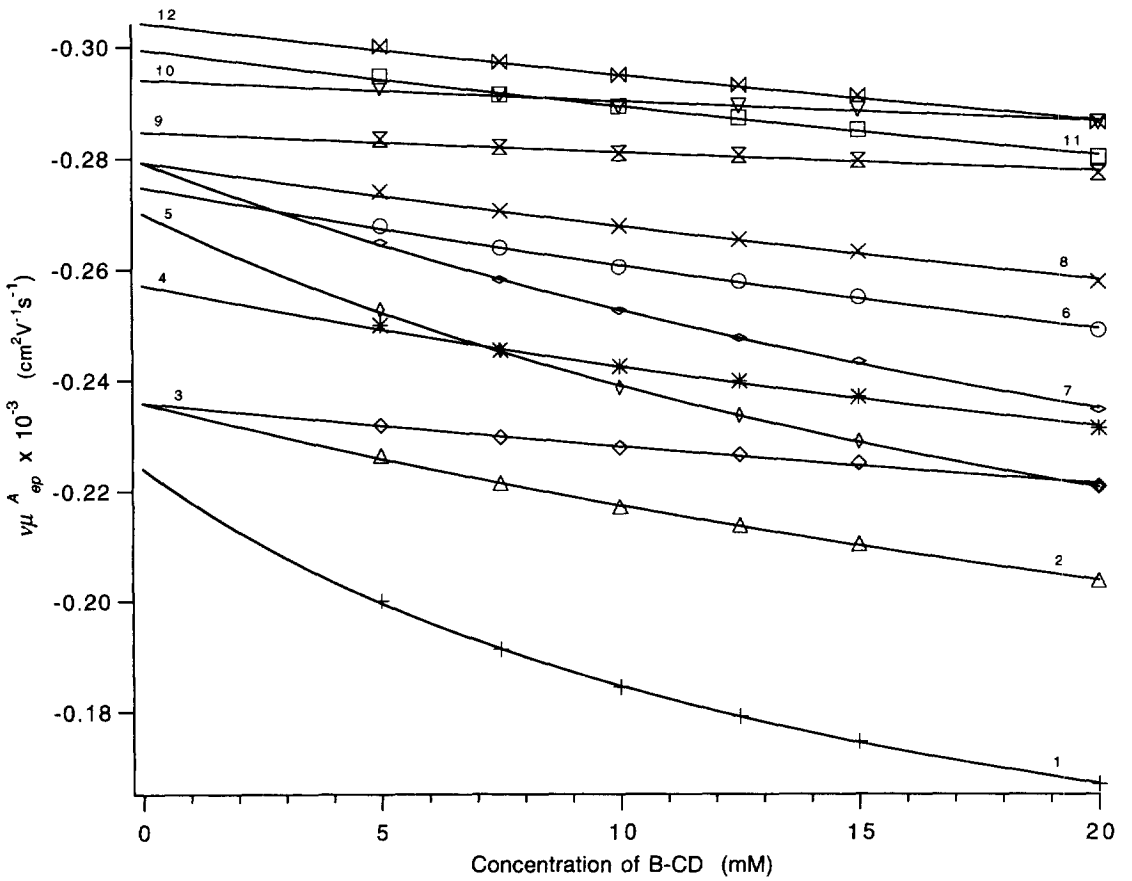

Fig. 3. Simulated ideal electrophoretic mobilities (solid lines) of 12 deoxyribonucleotides as a function of [β-CD] based on the fundamental parameters ($\mu_{ep,A}$, $\mu_{ep,AC}$ and K values) using Eq. (1). The markers represent the average measured mobilities at 5, 7.5, 10, 12.5, 15 and 20 mM β-CD. The nucleotides are numbered the same as in Fig. 1.

substantially, with peaks shifting at different rates and eventually overlapping and passing analytes that were originally eluted earlier. It is important to simultaneously model the migration behavior of all the analytes to choose the optimum separation conditions.

In order to translate the ideal state mobilities into migration times, the relative viscosity of the buffer solution and its electroosmotic mobility have to be considered. With the values shown in Fig. 3 and the viscosity correction, the migration times of all 12 deoxyribonucleotides can be plotted as a function of the β-CD concentration, as shown in Fig. 4. Again, there is excellent correlation between simulated migration times (solid curves) and measured average migration times, with a relative error of less than 1.5%. The plots of the simulated migration time can be used to predict the concentration of β-CD (14 m*M* in this case) required to achieve optimum separation.

The goal of this work was to verify that the plots in Figs. 3 and 4 can be used to accurately predict the analyte migration behavior at any usable concentration of β-CD under a variety of conditions. The calculated and experimental mobilities and migration times of all 12 deoxyribonucleotides were compared at β-CD concentrations of 2.5, 6, 14 (separation optimization) and 17.5 m*M*. These concentrations were chosen since they were not used originally in the model and encompass a wide range of β-CD concentrations. Excellent agreement between pre-

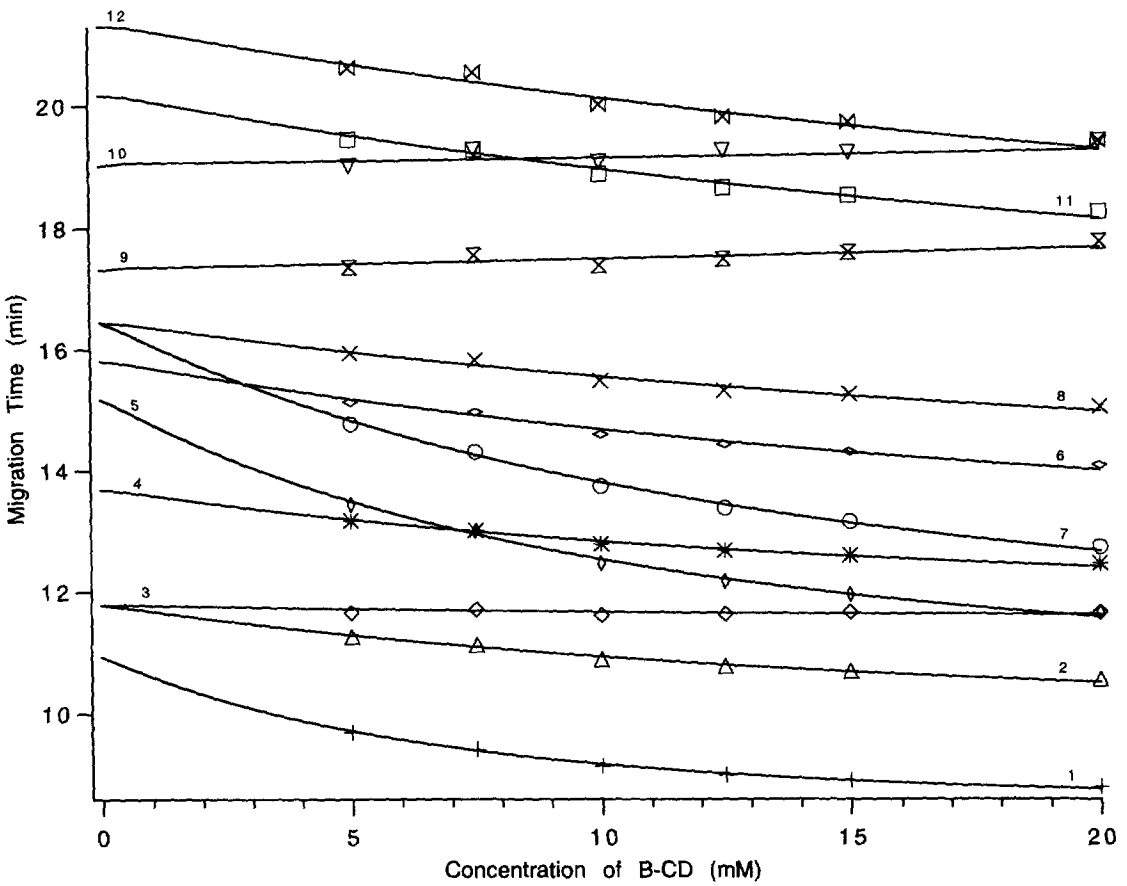

Fig. 4. Simulated apparent migration times (solid lines) of 12 deoxyribonucleotides as a function of β-CD concentration as predicted by the fundamental parameters ($\mu_{ep,A}$, $\mu_{ep,AC}$, K values), the viscosity correction factor (ν), and electroosmotic mobility (μ_{eo}). The markers represent the average measured migration times at 5, 7.5, 10, 12.5, 15 and 20 m*M* β-CD. The nucleotides are numbered the same as in Fig. 1.

Table 2
Prediction capablilities of theoretical model under various constraints

Constraint	Correlation plots — predicted vs. observed		N Number of data points	Rel. % error
	(A) For mobilities	(B) For migration times		
1. Same capillary (27 cm)/same buffer	$y=0.9968x+0.0002$ $R^2=0.9998$	$y=0.9854x+0.1411$ $R^2=0.9995$	144	0.1–0.9% 0.1–1.2%
2. Different capillary (27 cm)/new buffer	$y=0.9979x-0.0001$ $R^2=0.9992$	$y=0.9895x+0.074$ $R^2=0.9987$	72	0.1–1.0% 0.2–2.0%
3. Capillary length				
37 cm	$y=0.9979x-0.0001$ $R^2=0.9992$	$y=1.0017x-0.0252$ $R^2=0.9987$	72	0.2–1.1% 0.1–1.5%
47 cm	$y=0.9937x+0.0017$ $R^2=0.9986$	$y=1.0089x-0.1586$ $R^2=0.9987$	72	0.1–1.2% 0.2–1.3%

dicted and observed mobilities and migration times is shown (Table 2) by the linearity of the correlation plots and the low relative error. The migration time predictions have a slightly larger error than the mobility predictions. This is reasonable because the electroosmotic mobility often varies from run to run. Fig. 5(A) shows the separation optimization of all 12 dNPs at the predicted optimum condition (14 m*M* β-CD). The predicted migration times (marked by × in Fig. 5) of all 12 dNPs agree well with the obtained electropherogram.

4.4. Predictions using a different capillary and a different batch of buffer

Because the values of $\mu_{ep,A}$, $\mu_{ep,AC}$ and K are intrinsic properties of the analyte molecules and their environment [4], they should remain constant in a different capillary or in a new batch of buffer. A new batch of borate buffer with 6 and 14 m*M* β-CD was used to verify the calculated parameters. It was observed that the electroosmotic mobilities were 1 to 2% lower, and the currents were 0.8 to 1.0 μA lower than in the original buffer and capillary system. Despite these differences, the overall appearances of the electropherograms were similar. There is excellent correlation between the theoretical and the observed mobilities (Table 2). The relative error between the measured and the predicted mobilities is under 1%. In order to predict the migration times of the 12 dNPs, the average measured electroosmotic mobilities of the new solutions were used. Again, excellent correlation was observed between predicted and measured migration times, with a relative error ranging from 0.2 to 2.0%. Therefore, this dynamic complexation model is able to accurately predict the mobilities and migration times of analytes, even when the buffer and capillary are changed.

4.5. Predictions using different capillary lengths

Capillary lengths of 47 and 37 cm were used with the new buffer solutions to determine whether the model can still accurately describe the migration behavior of analytes. Voltages of 6.85 and 8.70 kV were applied to 37 and 47 cm long capillaries so that the electric field is the same as in the other experiments. An advantage of using longer capillary lengths is that analytes spend a longer time in the electric field, resulting in an increased difference in migration times. Correlation plots of electrophoretic mobilities and migration times for 6 and 14 m*M* β-CD solutions for both the 37 and 47 cm capillaries revealed a high degree of correlation between observed and predicted values (see Table 2). Fig. 5(B) and Fig. 5(C) show the electropherograms of the 12 dNPs at 14 m*M* β-CD using the 37 cm and the 47 cm capillaries. The predicted migration times of the dNPs agree well with those measured from the electropherograms (a relative error of less than 1.5%).

5. Conclusion

Analyte migration behavior can be quantitatively

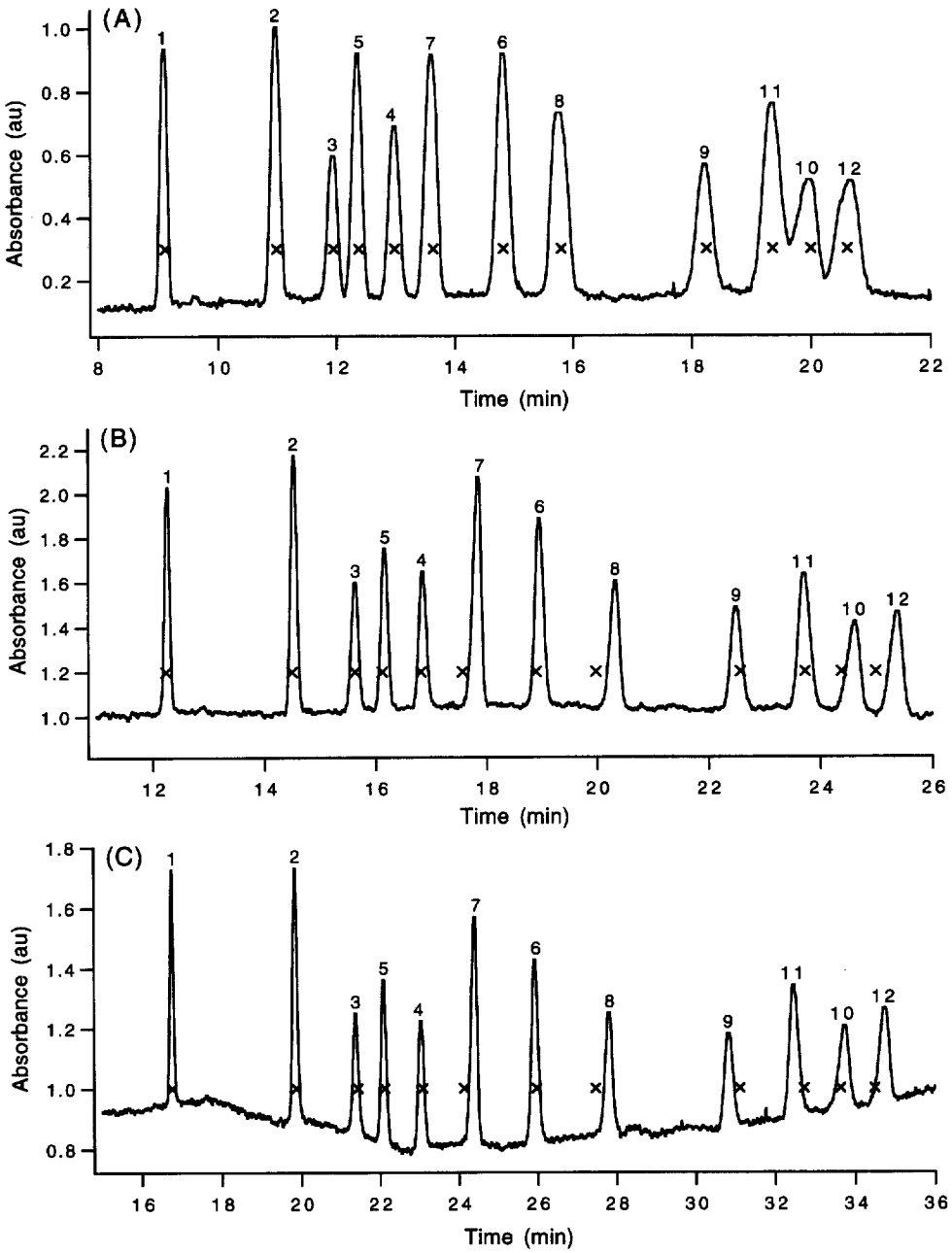

Fig. 5. Comparison between the migration times of various components in the electropherograms and the predicted migration times (×), showing the separation optimization of 12 deoxyribonucleotides at 14 m*M* β-CD using an (A) 27 cm, (B) 37 cm and (C) 47 cm capillary. The nucleotides are numbered the same as in Fig. 1.

described using the dynamic complexation model. The model was tested using different batches of buffer, different capillaries and different capillary lengths. It was concluded that this model can predict the electrophoretic mobility and migration time of an analyte when the temperature and pH are well

controlled. The three parameters: $\mu_{ep,A}$, $\mu_{ep,AC}$ and K, in conjunction with viscosity correction, can be used to systematically design a separation. Optimum separation conditions can be determined by simulating the migration time (or electrophoretic mobility) as a function of additive concentration, and selecting a concentration that produces the least overlap of migration time or mobility values. This understanding leads to more efficient method development through the selection of additives based on their affinity for the analytes, the mobility of the complexes and the optimum concentration(s) of the additive. Electrophoretic parameters and equilibrium constants, combined with molecular modeling, can assist in the design of CE separation systems.

Acknowledgements

The authors thank Naveen Chopra and Dr. John Sherman for the molecular modeling program and helpful discussions. This work is supported by the Department of Chemistry, University of British Columbia, and the Natural Sciences and Engineering Research Council of Canada. Beckman Instruments (Canada) Inc. kindly loaned us the P/ACE 5500 automated CE system used in this work.

References

[1] S.A.C. Wren, R.C. Rowe, J. Chromatogr. 603 (1992) 235–241.
[2] A. Shibukawa, D.K. Lloyd, I.W. Wainer, Chromatographia 35 (1993) 419–429.
[3] S.G. Penn, E.T. Bergström, D.M. Goodall, Anal. Chem. 66 (1994) 2866–2873.
[4] X. Peng, M.T. Bowser, P. Britz-Mckibbin, G.M. Bebault, J. Morris, D.D.Y. Chen, Electrophoresis 18 (1997) 706–716.
[5] M.T. Bowser, E.D. Sternberg, D.D.Y. Chen, Electrophoresis 18 (1997) 82–91.
[6] S. Terabe, K. Otsuka, K. Ichikawa, A. Tsuchiya, A. Teiichi, Anal. Chem. 56 (1984) 111–113.
[7] M.M. Rogan, K.D. Altria, D.M. Goodall, Electrophoresis 15 (1994) 808–817.
[8] S.G. Penn, D.M. Goodall, J. Chromatogr. 636 (1993) 149–152.
[9] C.L. Copper, J.B. Davis, R.O. Cole, M.J. Sepaniak, Electrophoresis 15 (1994) 785–792.
[10] Y.Y. Rawjee, G. Vigh, Anal. Chem. 66 (1994) 619–627.
[11] S.A.C. Wren, R.C. Rowe, R.S. Payne, Electrophoresis 15 (1994) 774–778.
[12] S. Terabe, K. Otsuka, A. Teiichi, Anal. Chem. 57 (1985) 834–841.
[13] N.H.H. Heegaard, J. Chromatogr. A 680 (1994) 405–412.
[14] S. Honda, A. Taga, K. Suzuki, S. Suziki, K. Kakehi, J. Chromatogr. 597 (1992) 377–382.
[15] J. Liu, K.J. Volk, M.S. Lee, E.H. Kerns, I.E. Rosenberg, J. Chromatogr. A 680 (1994) 395–403.
[16] S. Terabe, H. Ozaki, K. Otsuka, T. Ando, J. Chromatogr. 332 (1985) 211–217.
[17] K. Ghowsi, J.P. Foley, R.J. Gale, Anal. Chem. 62 (1990) 2714–2721.
[18] M.G. Khaledi, S.C. Smith, J.K. Strasters, Anal. Chem. 63 (1991) 1820–1830.
[19] J.K. Strasters, S. Kim, M.G. Khaledi, J. Chromatogr. 586 (1991) 221–232.
[20] C. Quang, M.G. Khaledi, J. Chromatogr. A 659 (1994) 459–466.
[21] R.S. Sahota, M.G. Khaledi, Anal. Chem. 66 (1994) 2374–2381.
[22] S.G. Penn, E.T. Bergström, I. Knights, G. Liu, A. Ruddick, D.M. Goodall, J. Phys. Chem. 99 (1995) 3875–3880.
[23] K.L. Rundlett, D.W. Armstrong, J. Chromatogr. A 721 (1996) 173–186.
[24] K.A. Conners, Binding Constants — The Measurement of Molecular Complex Stability, Wiley, Toronto, 1987.
[25] Handbook of Biochemistry: Selected Data for Molecular Biology, CRC Press, Cleveland, OH, 1970.
[26] C. Formoso, Biochem. Biophys. Res. Commun. 50 (1973) 999–1005.
[27] J.L. Hoffman, R.M. Bock, Biochemistry 9 (1970) 3542–3550.
[28] M. Uhrová, Z. Deyl, M. Suchánek, J. Chromatogr. B 681 (1996) 99–105.
[29] T. Tadey, W.C. Purdy, J. Chromatogr. B 657 (1994) 365–372.
[30] R.E. Offord, Nature 211 (1966) 591–593.